A Molecular-Scale Model for the Coupling of Heat and Matter Fluxes at a Gas−Liquid Interface

Leon F. Phillips

Chemistry Department, University of Canterbury, Private Bag 4800, Christchurch, New Zealand

Received: December 19, 2002; In Final Form: June 2, 2003

The phenomena that are encapsulated in the Onsager heat of transport at a liquid−vapor interface are modeled in terms of processes occurring in the capillary-wave zone at the liquid surface. The effect of localized heat release in the outer part of the capillary-wave zone is in the right direction but is too small to account for the observations. A more successful approach considers the effect of a temperature gradient on the effective barrier height for escape from the liquid. The results imply that evaporating molecules must surmount a free-energy barrier rather than an enthalpy barrier and that the detailed dynamics of barrier crossing play an important role.

Introduction

The flux, J, of gas through a region in which there are simultaneous fluxes of heat and matter is given by the equation

$$J = -\frac{L_{22}}{\delta}\left(\frac{Q^*}{RT}\frac{\Delta T}{T} + \frac{\Delta P}{P}\right) \tag{1}$$

where δ is the width of the (narrow) region across which the temperature and pressure changes are ΔP and ΔT, R is the ideal gas constant, and Q^* is the Onsager heat of transport.[1−3] The requirement that eq 1 should reduce to Fick's law of diffusion in the absence of a temperature gradient allows us to identify the coefficient L_{22} as the product of the average diffusion coefficient D and concentration C in the narrow region, where $\Delta P/P = \Delta C/C$. The relative importance of the temperature and pressure gradients in deciding the magnitude and direction of the gas flux depends on the factor $Q^*/(RT)$.

In practice, Q^* is obtained from the stationary-state equation

$$\frac{Q^*}{RT} = -\frac{\Delta P}{P}\frac{\Delta T}{T} \tag{2}$$

which holds when the flux of matter is zero.[4−6] In our work, we apply a known temperature gradient across a thin layer of gas adjacent to the liquid surface and measure the effect on the stationary-state vapor pressure. Initial experiments with aniline showed that Q^* is of similar magnitude to the latent heat of vaporization, so $Q^*/(RT)$ is usually greater than 10, Q^* decreases with increasing δ, but the effect of Q^* is still significant for values of δ greater than 30 mean free paths in the gas phase, and a positive temperature gradient results in a positive pressure change, which means that the sign of Q^* is negative.[6] The dependence of ΔP on ΔT was found to be nonlinear for values of ΔT greater than about 0.5 K, so Q^* had to be determined from the initial slopes of plots of ΔP versus ΔT. The triple-point vapor pressure of aniline is such that the lowest accessible value of δ corresponded to about eight mean free paths.

Recent work with *n*-heptanol,[7] which has a much lower triple-point pressure, has shown that linear plots are obtained up to ΔT at least 3 K when δ is less than one mean free path. The nonlinear and linear regimes actually overlapped, which strongly suggests that the nonlinearity is an artifact, due probably to the presence of unintended horizontal components in the vapor-phase temperature gradients. Experiments in progress aim to eliminate the presumed artifact and to determine the range of ΔT over which eq 2 remains valid.

If Q^* is defined as the heat that is absorbed on one side of the region and released on the other, the observation that Q^* is negative requires that positive fluxes of heat and matter and positive gradients of temperature and pressure are directed *away* from the liquid. The present paper shows that this requirement can be understood in terms of a mechanism based on the effect of the temperature gradient on the effective height of the free-energy barrier to evaporation. The observation that Q^* continues to increase with decreasing δ for values of δ less than a mean free path rules out a purely gas-phase origin for the effects that we observe.[8] Our initial experiments also revealed the apparently paradoxical phenomenon of a cool liquid distilling onto a warmer surface[9] and provided indirect experimental support[8] for the well-known theoretical paradox[10] of inverted gas-phase temperature gradients during trap-to-trap distillation.

The trivial explanation of these observations, that the pressure increases were due to gross heating of the liquid surface, is ruled out by the observed dependence[6] of Q^* on δ and by the fact that in these experiments the temperature of the liquid was thermostatically controlled by reference to a thermistor immersed in the surface layer. Theoretical studies using either Boltzmann equation[10] or irreversible thermodynamic treatments[11] of the Knudsen layer adjacent to the surface appear not to predict either the effect of the temperature gradient on the gas pressure or the consequent phenomenon of a cool liquid distilling onto a warmer surface. However, it appears likely that further analysis will show that this phenomenon and the paradox of inverted temperature profiles are merely two sides of the same coin.

For a system comprising two gas−liquid interfaces, as shown diagrammatically in Figure 1, Spanner[3] used Onsager's equations for the fluxes of heat and matter to deduce that, for small values of ΔP and ΔT, the heat of transport Q^* for the process of transferring material from liquid reservoir 1 to liquid reservoir 2 should be given by eq 2 with $|Q^*|$ equal to the latent heat of vaporization. If we imagine this system to be split into two

10.1021/jp027777u CCC: $25.00
Published on Web 07/25/2003

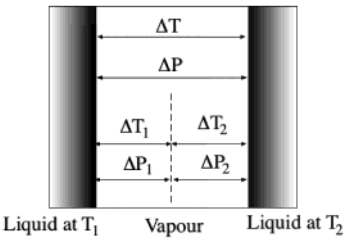

Figure 1. Decomposition of the two-surface system of Spanner[3] into a pair of gas−liquid interfaces.

halves, as indicated by the dashed line and assume that the vapor-phase gradients of temperature and pressure are constant, each half corresponds to the kind of system studied in our experiments and eq 2 applies to each half of the system separately with the same value of Q^* and with (ΔP_1, ΔT_1) or (ΔP_2, ΔT_2) replacing (ΔP, ΔT). Spanner's main concern was the possibility that significant pressure differences might be generated by small temperature differences in biological systems. His work appears to have been overlooked by physical chemists, and his predictions were not tested by experiment.

The current view of the gas−liquid interface is that the liquid surface is sharply defined at any instant but is highly mobile with a surface roughness that increases markedly when the scale of observation is reduced to molecular dimensions.[12] The rate of change of the surface displacement with time and the height−height correlation over distances on the order of two or three molecular diameters are such that there is a well-defined surface slope with respect to the trajectories of incoming gas-phase molecules having kinetic energies on the order of 100 kJ mol^{-1} [13,14] but there is no well-defined surface slope on the time scale of an incoming molecule at thermal energies.[15,16] The motion of the surface results from the superposition of about 10^4 periodic normal modes and about 10^8 nonperiodic local modes having fast rise and slow fall times.[17] The changeover from normal to local modes occurs at the critical-damping wave vector, k_c ($=2\pi/\lambda_c$) given by

$$k_c = \rho\gamma/\eta^2 \tag{3}$$

where ρ is density, γ is surface tension, and η is viscosity. The rise and fall times are

$$\tau_{rise} = \rho/(2k^2\eta) \tag{4}$$

and

$$\tau_{fall} = 2\eta/(k\gamma) \tag{5}$$

respectively.

For aniline, taking the collision diameter as 5.4×10^{-8} cm on the basis of a comparison of the molecular volumes of aniline and benzene, for which the listed collision diameter is 5.27×10^{-8} cm, the maximum k value is 8.9×10^8 cm^{-1} and the value of k_c is 3.3×10^4 cm^{-1}. The degeneracy of a mode is expected[17] to be proportional to k^2, so local modes greatly outnumber the normal modes. The instantaneous value of the surface displacement from its mean position is normally distributed about zero, with an rms displacement of 4.0×10^{-8} cm for an aniline surface at 300 K, about 2.6×10^{-8} cm of this rms displacement being attributable to local modes.

If we use a simple Stokes' law calculation to estimate the retarding force on an incoming molecule, the stopping time, defined as the time for the molecule's velocity to be reduced to 10% of its initial value by viscosity, is independent of the initial

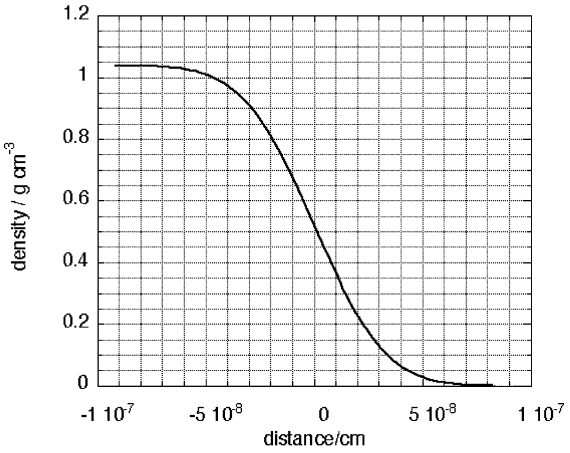

Figure 2. Variation of the time-averaged density of aniline with distance with the location of the mean surface as origin and considering only the time variation due to rising phases of the local modes.

velocity. For aniline, the results are 4.7 ps for viscosity equal to that of the vapor and 5.8 fs for viscosity equal to that of the liquid. The stopping time for a molecule in the capillary-wave zone must lie somewhere between these extremes. The k values for which the rise time of a local mode is equal to the stopping time are 1.1×10^5 cm^{-1} for the gas and 3.2×10^6 cm^{-1} for the liquid. Both of these values are near the lower end of the local mode spectrum, so we can assume that the main interaction is with time-averaged local modes, the normal modes being effectively frozen out, and that the majority of local modes have rise times that are very fast in comparison with the time required for a molecule to lose 90% of its velocity, that is, 99% of its kinetic energy. However, the fall times for local modes are so much longer than the rise times that the corresponding k values, 1.1×10^9 cm^{-1} for the gas and 9×10^{11} cm^{-1} for the liquid, are outside the available range for an aniline surface. Hence, on the time scale of an encounter with an incoming molecule, the recovery phase of the local modes is also frozen out. The displacement corresponding to the rising phase of a local mode can be either positive or negative, so an incoming molecule experiences very rapid, random displacements of the surface due to superposition of the "rising" phases of many different local modes.

The conclusion that the surface motion is very rapid on the scale of the stopping time of an incoming molecule at room temperature suggests that the time-averaged interaction of the molecule and the surface can be calculated using time-averaged values of such quantities as density, heat capacity, entropy, chemical potential, and thermal conductivity. In other words, these quantities can be assumed to vary continuously between the liquid-phase and gas-phase values as the point of observation moves through the capillary-wave zone. That is the basic assumption of the present calculations.

Calculations and Results

1. The Effect of Local Heat Release on the Evaporation Rate. The calculations used an evenly spaced 201-point grid to cover the range from liquid to vapor. Because the location of the surface is normally distributed about its mean value, the bulk properties can be scaled to erf(z) or erfc(z) functions of distance z between the liquid- and gas-phase values, where the erf(z) functions are derived from a normal distribution of which the width corresponds to the root-mean-square displacement of the surface. Figure 2, a plot of aniline density versus distance

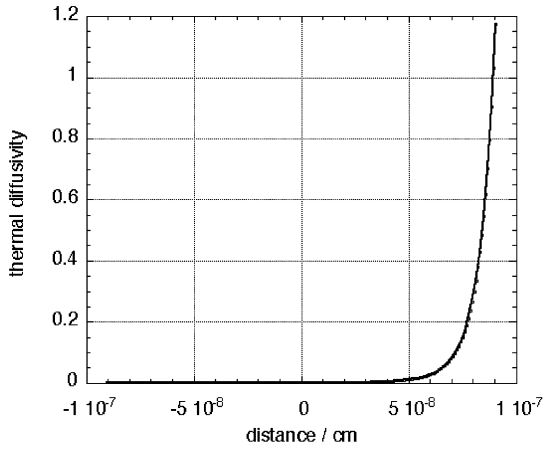

Figure 3. Variation of thermal diffusivity with distance, calculated as in Figure 2.

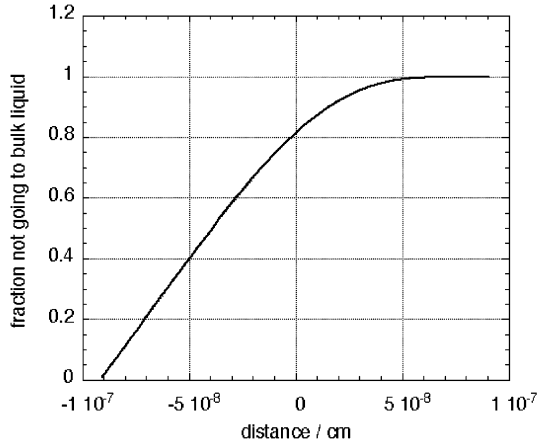

Figure 4. Fraction of local heat release not being conducted into the bulk liquid, calculated as in Figure 2.

measured from the mean surface, is a typical graph. The effective thickness of the mobile zone is seen to be about 10^{-7} cm.

Figure 3, which is a graph of thermal diffusivity (thermal conductivity divided by the product of density and heat capacity) versus distance, shows that temperature changes due to a local release of heat are most readily propagated through the less dense region far from the surface. By calculating the integrals of the reciprocal of thermal diffusivity over distance to the bulk gas and liquid regions for each point in the mobile zone, we obtain Figure 4, which shows, as a function of distance, the fraction of locally released heat that does not enter the bulk liquid. To estimate the rate of kinetic energy plus latent heat release due to incoming molecules as a function of distance, we first assume that molecules leaving a solid plate a few millimeters above the surface have a Maxwell distribution of velocities characteristic of the temperature of the plate and that the emission rate has a cos θ angular distribution, where θ is the angle between the velocity vector and the normal. We continue to assume that the molecules arriving at the surface lose their velocity in accordance with Stokes' law and that a fraction of the latent heat proportional to the local density is released when a molecule has lost 99% of its kinetic energy. We also assume, on the basis of the principle of detailed balance, that the same fraction of the latent heat is required to cause evaporation of the same or a different molecule from the point where the incoming molecule was effectively stopped. The stationary-state pressure is then calculated by requiring the total evaporation rate to equal the condensation rate, and this is done for a range of temperatures of the plate.

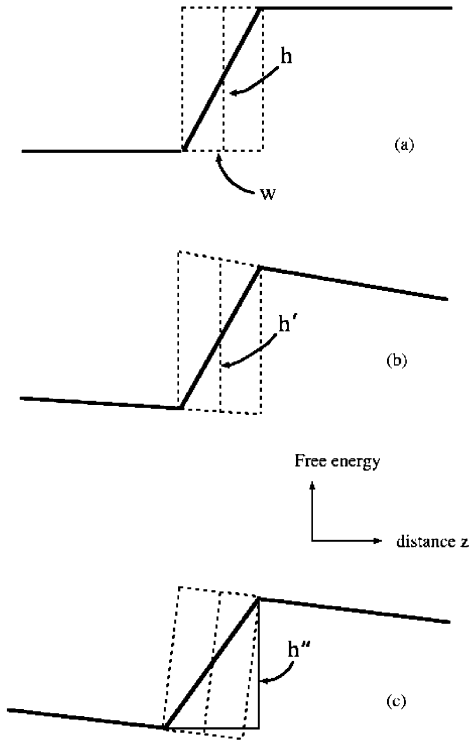

Figure 5. Free-energy barriers to evaporation: (a) with no superimposed temperature gradient; (b) the adiabatic limit with a positive temperature gradient leading to negligible change in barrier height; (c) the dynamic, or diabatic, limit with a positive temperature gradient leading to a reduction in barrier height.

Calculations of this sort do predict a pressure increase in the same direction as that observed when the temperature of the heated plate is raised, but the size of the predicted effects, which correspond to heats of transport of 2 kJ mol^{-1} or less, is more than an order of magnitude too small to account for the observations. Hence, we conclude that local heating of the surface is not the origin of the effects reported in ref 6.

2. The Effect of a Temperature Gradient on the Height of the Barrier to Evaporation. The sign of the effect of a temperature gradient on the height of a barrier to evaporation depends on the nature of the barrier. For an enthalpy barrier, the effect will depend on $\partial H/\partial T = C_p$, which is positive. For a free-energy barrier, the effect will depend on $\partial G/\partial T = -S$, which is negative. The experimental results correspond to the situation in which a positive temperature gradient (temperature increasing from liquid to gas) lowers the barrier, so we conclude that the barrier of interest is a free-energy barrier. Hence, if h is the barrier height, we can write $\partial h/\partial z = (\partial h/\partial T)(\mathrm{d}T/\mathrm{d}z) = -S(\mathrm{d}T/\mathrm{d}z)$, where the free energy and entropy are molar quantities, so h is actually the chemical potential, and the distance z is measured through the capillary-wave zone in the direction from liquid to gas. In a stationary state, with constant heat flux, the temperature gradient varies with z in proportion to $1/\kappa$, where the variation of the conductivity κ with distance is similar to the variation of density that is shown in Figure 2. We now consider two extreme cases. Because we are dealing with macroscopic thermodynamic properties, the diagrams that follow must relate to ensemble averages.

Figure 5a shows an unperturbed free-energy barrier to evaporation, where the height h of the barrier is given by the length of the central vertical line in the small rectangle that contains the transition region. In Figure 5b,c a free-energy

TABLE 1: Values of the Heat of Transport Q^* Calculated at the Dynamic Limit for Liquid Temperature 270 K, with Barrier Height $h \cos \phi$, Where $\phi = \tan^{-1}(S\ (dT/dz))$

T (K) top plate	Q^* (kJ mol^{-1}) midpoint[a]	Q^* (kJ mol^{-1}) weighted average[b]
270.0		
270.1	17.1	120.9
270.2	35.4	234.3
270.3	54.0	335.4
270.4	72.8	425.4
270.5	92.1	506.8

[a] Uses cos ϕ evaluated at the mean surface. [b] Uses a weighted average of cos ϕ over the whole capillary-wave zone.

gradient, $-S(dT/dz)$, has been applied to the diagram. In Figure 5b, the rectangle is distorted into a trapezium, so the once-horizontal boundaries now have the same slopes as the lines leading to and from the former rectangle and the slopes of the vertical lines are essentially unchanged. In Figure 5c, the whole diagram has been rotated so that the rectangle is undistorted. Figure 5b corresponds to what might be termed the *adiabatic* limit, in which an escaping molecule experiences the time-averaged free-energy barrier and the effective barrier height h' becomes approximately $h + w(S_{liq} + S_{gas})(dT/dz)/2$, where w is the effective thickness of transition region, which is at most equal to the thickness of the mobile zone. Because w is very small ($\sim 10^{-7}$cm) and dT/dz is only on the order of unity, the effect of the temperature gradient on the barrier height is negligible in this case.

Figure 5c corresponds to what might be termed the *dynamic* or *diabatic* limit, such that an escaping molecule takes a very short time to achieve the separation from nearest neighbors that corresponds to crossing the barrier, so the effective thickness of the transition region is very small. In this limit, shown in Figure 5c, the effective height of the free energy barrier is $h'' = h \cos \phi - w \sin \phi \approx h \cos \phi$, where ϕ is $\tan^{-1}(S(dT/dz))$, and S is now the local value of entropy, which can be assumed to scale approximately as erf(z).

Typical results of calculations at the dynamic limit with $h'' = h \cos \phi$ are given in Table 1 for a liquid temperature of 270 K and with plate temperatures as shown in column 1 of the table. Column 2 contains values of the resulting heats of transport Q^* with ΔP calculated using the temperature gradient and entropy values at the mean surface. Column 3 contains values of Q^* for which the entropy and temperature gradient were weighted averages evaluated over a range of distances, which were normally distributed around the location of the mean surface. The two sets of Q^* values differ by about a factor of 5, which shows that the choice of averaging procedure has a major effect on the outcome of the calculation. Both calculations yield values that increase with increasing ΔT, which is contrary to observation. If this aspect of the model is correct, the results imply that the relative contribution of the diabatic and adiabatic limiting cases varies with ΔT in a manner that corresponds to the average width of the transition region increasing with increasing temperature gradient. The two smallest values in column 2 are less than the experimental value of around 50 kJ mol^{-1}. The other values in column 2 and all of the values in column 3 are larger than the experimental value. Thus, this mechanism with weighted averages of the entropy and temperature gradient is capable of accounting for the observed phenomena provided that we assume that the detailed dynamics of barrier crossing plays an important part and that the relative contributions of adiabatic and diabatic limiting cases varies quite strongly with ΔT. Full trajectory calculations are needed to establish whether this picture is truly viable, as opposed to merely plausible.

Acknowledgment. The author gratefully acknowledges the support of the U.S. National Science Foundation (Grant No. 0209719).

References and Notes

(1) Denbigh, K. G. *The thermodynamics of the steady state*: Methuen, London, 1951.
(2) Spanner, D. C. *Symp. Soc. Exp. Biol.* **1954**, *8*, 76.
(3) Phillips, L. F. *J. Chem. Soc., Faraday Trans.* **1991**, *87*, 2187.
(4) Denbigh, K. G.; Raumann, G. *Proc. R. Soc. (London)*, **1952**, *A210*, 377.
(5) Denbigh, K. G.; Raumann, G. *Proc. R. Soc. (London)* **1952**, *A210*, 518.
(6) Mills, C. T.; Phillips, L.F. *Chem. Phys. Lett.* **2002**, *366*, 279.
(7) Mills, C. T.; Bones, D. L.; Casavecchia, P.; Phillips, L. F. *Phys. Chem. Chem. Phys.*, submitted for publication.
(8) Mills, C. T.; Phillips, L. F. *Chem. Phys. Lett.* **2003**, *372*, 609.
(9) Mills, C. T.; Phillips, L. F. *Chem. Phys. Lett.* **2003**, *372*, 615.
(10) Pao, Y. P. *Phys. Fluids* **1971**, *14*, 306.
(11) Bedeaux, D.; Hermans, L. J. F.; Ytrehus, T. *Physica A* **1990**, *169*, 263.
(12) Fradin, C.; Braslau, A.; Luzet, D.; Smilgies, D.; Alba, M.; Boudet, M.; Mecke, K.; Daillant, J. *Nature* **2000**, *403*, 871.
(13) Fiehrer, K. M.; Nathanson, G. M. *J. Am. Chem. Soc.* **1997**, *119*, 251.
(14) Knox, C. J. H.; Phillips, L. F. *J. Phys. Chem. B* **1998**, *102*, 10515.
(15) Phillips, L. F. *Chem. Phys. Lett.* **2000**, *320*, 398.
(16) Somasundaram, T.; Lynden-Bell, R. M.; Patterson, C. H. *Phys. Chem. Chem. Phys.* **1999**, *1*, 143.
(17) Phillips, L. F. *J. Phys. Chem. B* **2001**, *105*, 11283.